Transactions of the Nigerian Association of Mathematical Physics
Volume 5,(September and November, 2017), **pp127 –140**

Variable Viscosity, Nonlinear Thermal Radiation And Slip Effects On Unsteady MHD Micropolar Fluid in a Porous Medium in the Presence of Thermophoresis and Ohmic Heating

Yusuf T. A. and Gbadeyan J. A.

Department of Mathematics, University of Ilorin, Ilorin, Nigeria

Abstract

In this study, the effect of variable viscosity, Soret number and non-linear thermal radiation on an unsteady hydromagnetic mixed convection heat and mass transfer of a micropolar fluid past a vertical stretching sheet through a porous medium with slippage, thermophoresis, Ohmic heating and heat source is investigated. An optically thick limit approximation for radiation heat flux is assumed. The governing boundary layer equations for the model are reduced using similarity transformation to a set of coupled nonlinear ordinary differential equations The transformed equations are then integrated numerically using the fourth-fifth order Runge-Kutta-Fehlberg integration scheme. Influence of various physical parameters on the dimensional velocity, microrotaion, temperature, concentration, velocity gradient, wall coupled stress, temperature gradient and concentration gradient are shown graphically and discussed in detail. The results obtained are compared with those from previous studies and found to be in good agreement. It is noticed that the rate of heat transfer at the surface decelerates with an increase in a thermophoretic parameter, while the reverse is noticed for the local Sherwood number.

Keyword: Micropolar fluid, slip condition, porous medium, thermophoresis, nonlinear thermal radiation

Nomenclature

: Unsteadiness parameter
a: Constant $[m^{-1}]$
b: Constant $[m^{-1}\theta]$
B_0: Magnetic field strength
Cf_x: Coefficient of local skin-friction
C_p: Specific heat at constant pressure$[JKg^{-1}\ K^{-1}]$
C: Concentration of the fluid
C_w: Wall concentration
C_∞: Concentration of the fluid far away from the sheet
D_m: Coefficient of mass diffusivity
Ec: Eckert number
f: Non-dimensional velocity component
g: Acceleration due to gravity $[m^{-2}]$
s: Non-dimensional velocity slip
Gr: Grashoff number for heat transfer
Gm: Grashoff number for mass transfer
j: Microinertia density
k_0: Permeability of the porous medium
k_1: Rosseland mean absorption coefficient$[m^{-1}]$
k_∞: Thermal conductivity of the fluid$[Wm^{-1}\ K^{-1}]$
L: Dimensional slip parameter
H: Magnetic field
N: Dimensional Microrotation component$[rad\ s^{-1}]$
R: Thermal radiation parameter

Correspondence Author: Yusuf T.A., E-mail: tundeayusuf04@gmail.com, Tel: +2348038585662

Nu_x: Nusselt number
p: Pressure$[Nm^{-2}]$
Pr: Prandtl number
Q_0: Heat source parameter
q_m: Mass flux at the wall$[ms^{-1}]$
q_r: Radiative heat flux $[Wm^{-2}]$
Re_x: Local Reynolds number
s: Dimensionless velocity slip parameter
Sc: Schmidtl number
So: Soret number
Sh_x: Local Sherwood number
t: time$[s]$
T: Temperature $[K]$
T_f: Reference temperature
T_r: Temperature ratio parameter
T_w: Wall temperature [K]
T_∞: Temperature of the fluid far away from the sheet$[K]$
u, v: Velocities in x and y directions$[m^{-1}]$
x, y: Axial and perpendicular coordinates $[m]$.

Greek Symbols
δ: Permeability parameter
β: Material parameter
μ: Dynamic viscosity
σ_1: Stefan–Boltzmann constant
β_1: Volumetric coefficient of the thermal expansion$[K^{-1}]$
β_2: Volumetric coefficient of the concentration expansion
η: Non-dimensional distance
φ: Porosity of the porous medium
υ: Kinematic viscosity $[m^2\ s^{-1}]$
ρ: Fluid density $[kgm^{-3}]$
θ: Non-dimensional temperature
σ: Electrical conductivity of the fluid
ϕ: Non-dimensional concentration
α: Variable viscosity parameter.
κ: Vortex viscosity
τ: Thermophoresis parameter
Subscripts
∞: Free stream condition
w: Condition at the wall of stretching sheet.
Superscript
: Derivative with respect to

Introduction

The study of heat and mass transfer of fluid flow over a stretching sheet has recently gained interest of a number of researchers due to its vast application in engineering and industries, this include, the production of glass fiber and polymer sheets, the cooling and drying of paper and textiles and a lot more. It is also applicable especially in many metallurgical processes that involve cooling of continuous strips or filament by drawing them through a quiescent fluid and in the process of drawing, these filaments are sometimes stretched. Other related applications can be found in Refs [1-2].

Micro fluids are those which contain micro-constituents and can undergo rotation. The theory of micropolar fluid model introduced in [3] exhibits the local effect arising from the micro structure and micro motion of the fluid elements. Its practical application includes colloidal suspension, solidification of liquid crystals, extrusion of polymer fluids, animal blood etc. This type of fluid has been studied by many researchers in various geometries. Some important contributions on micropolar fluid flow over a stretching surface under different conditions include the work of [4] who investigated the flow of micropolar fluid past a porous stretching sheet. Rahman et al [5] also studied the heat transfer in micropolar fluid along a linear stretching sheet with temperature dependent viscosity and variable surface temperature. Lately, [6] studied the effect of chemical reaction and double stratification on MHD free convection in a micropolar fluid with heat generation and Ohmic heating. In another work of [7], effect of thermal radiation in mixed convention of a micropolar fluid from an unsteady stretching surface with viscous dissipation and heat generation/absorption has been analyzed.

The application of studies involving the flow of micropolar fluid through various porous media can be found in te production of aerogels, alloys, polymer blends and foamed solids. Turyilmazoglu [8] examined the flow of a micropolar fluid due to porous stretching sheet and heat transfer. Zaib and Shafie [9] studied the heat and mass transfer in a MHD non-Darcian micropolar fluid over an unsteady stretching sheet with non-uniform heat source/sink and thermophoresis.

Most flows of micropolar fluid have been studied under no-slip boundary condition. Slip phenomena occurrence of micropolar fluid on MHD mixed convection stagnation point flow towards a shrinking vertical sheet have been studied in [10]. Zaib and Shafie [11] also investigated the Slip effect on unsteady MHD stagnation-point flow of a micropolar fluid towards a shrinking sheet with thermophoresis.

Thermophoresis can be described as a mechanism at which colloidal particles migrate due to temperature gradient [12]. This phenomenon causes small particles to move away from a high temperature surface toward a low temperature surface. The velocity attained and the forces exerted by the suspended particles caused by change in temperature are known as thermophoretic velocity and thermophoretic forces respectively. Some of the practical applications of this mechanism are the removal of small particles from a gas particle trajectory in combustion devices, in the micro electronics manufacturing and in nuclear reactor safety. Talbot et al [13] investigated thermophoresis of particles in a heated boundary layer. In the work of [14] thermophoresis deposition of particles in laminar and turbulent flows was examined. Effect of thermophoresis particle deposition in free convection boundary layer from a vertical flat plate embedded in a porous medium is studied by Chamkha and Pop [15]. Recently, [12] analyzed thermophoresis and MHD mixed convection three dimensional flow of viscous elastic fluid with Soret and Dufour effects using Homotopy analysis method. Other studies of mass and heat transfer characteristics of fluid flow over a stretching /shrinking surface with thermophoresis include those in [16-19].

All of the above mentioned studies considered mass and heat transfer of micropolar fluid flow in the presence of thermophoresis in various geometries with uniform viscosity. But in many practical situation, these physical properties changes significantly with the temperature. For example, the effect of thermophoresis and chemical reaction on MHD micro polar fluid flow with variable fluid properties is been studied in [20]. Furthermore, Saddeek [21] employed finite element method to analyze the effect of chemical reaction, variable viscosity, thermophoresis and heat and mass transfer over a heat surface. Rahmon et al [5] have also studied the heat transfer in micropolar fluid along a linear stretching sheet with temperature dependent viscosity and variable surface temperature.

The effect of thermal radiation has a vital role in the thermal performance of working fluids. Its importance is seen in variety of applications such as gas turbine, space technology, nuclear power plants and also processes in engineering field where high temperature is required. At high temperature, thermal radiation influences the heat transfer and temperature distribution of a fluid through different geometries. Mohamed and Ado-Dahab [22] investigated chemical reaction and thermal radiation effect on the heat and mass transfer in the MHD micropolar flow over a vertical moving porous medium with heat generation. Few studies in this direction are [7, 23-26]. All these aforementioned studies used the optically thick limit approximation to simulate the thermal radiation. They also assumed small temperature difference within the flow to linearize the radiative heat flux gradient. In other words they did not consider non-linear thermal radiation.

Convection problems associated with fluid flow, heat and mass transfer by involving non-linearized radiative heat flux gradient was carried out in [27] who studied the effect of thermal radiation on entropy generation due to micropolar fluid flow along a wavy surface. Uddin et al [28] discussed the radiative convective nanofluid past a starching/shrinking sheet with slip effects. Recently, [29, 30] have investigated the effect heat transfer of a radiative MHD fluid flow taking non-linear thermal radiation into consideration. They have all reported that the presence of nonlinear thermal radiation significantly influences the fluid temperature.

Mass diffusion due to temperature also known to be the Soret number effect has also had its relevance in industries. Studies of Soret effect in various convective flows include the work in Refs. [31-34]. However, none of these considered the effect of Soret and thermophoresis on micropolar fluid flow and heat transfer.

The aim of this work is therefore to study the effect of velocity slip and Soret number in hydro magnetic micropolar fluid flow in a porous medium over an unsteady vertical stretching sheet with Ohmic heating and thermophoresis. This problem is relevant in chemical engineering fluids including manufacturing of lubricants and polymeric suspensions. Here, the non linear radiation heat flux is adopted. The governing nonlinear partial differential equations are transformed to a set of non linear ordinary differential equation and then solved numerically by fourth-fifth order Runge-Kutta-Fehlberg scheme [35]. The effect of various controlling parameters (namely, variable viscosity parameter, Hartman number, solutal and thermal buoyancy parameters, velocity slip, Darcy number, radiation conduction, heat source parameter, Soret number, Schmidt number and thermophoretic parameter) on the dimensionless velocity, temperature, angular velocity and concentration profiles are graphically analyzed and represented in table.

Formulation of the problem

The heat and mass transfer of an unsteady two dimensional mixed convective boundary layer slip flow of a viscous incompressible electrically conducting micropolar fluid over an impermeable stretching sheet through a porous medium under the influence of thermophoresis, non-linear thermal radiation, heat source and transverse magnetic field is considered. The flow model is shown in Fig 1. The flow is assumed to be in positive x direction and this is taken along the plate while the positive y coordinate is normal to it. The flow taken w is caused by the stretching of the sheet which moves in its own plane with surface slip velocity U_w. A uniform magnetic field of strength B_0 is applied normally to the flow and the electrical conductivity is assumed to be constant. The Ohmic heating due to the application of magnetic field is also considered. The temperature dependent viscosity and the Darcy resistance terms are taken into account.

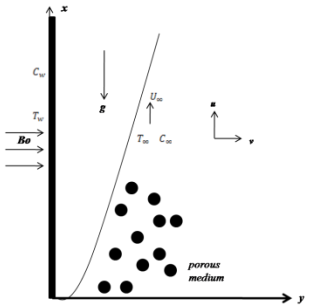

Fig 1. Physical model and coordinate system.

Furthermore, the surface temperature T_w of the stretching sheet is assumed to vary with distance x and time t, and T_∞ is the ambient fluid temperature. The Soret effect is also considered in this model.
Under these assumptions the unsteady boundary layer equations [7, 9] are
Continuity equation

$$\frac{\partial u}{\partial x}+\frac{\partial v}{\partial y}=0 \tag{1}$$

Momentum equation

$$\left(\frac{\partial u}{\partial t}+u\frac{\partial u}{\partial x}+v\frac{\partial u}{\partial y}\right)=\frac{\partial}{\partial y}\left(\left(\frac{\mu(T)+\kappa}{\rho}\right)\frac{\partial u}{\partial y}\right)-\left(\sigma B_0^2+\frac{\mu(T)\phi}{k_0}\right)u-\frac{\kappa}{\rho}\frac{\partial N}{\partial y}+g\beta_1(T-T_\infty)+g\beta_2(C-C_\infty) \tag{2}$$

Heat balance equation

$$\rho C_p\left(\frac{\partial T}{\partial t}+u\frac{\partial T}{\partial x}+v\frac{\partial T}{\partial y}\right)=k\frac{\partial^2 T}{\partial y^2}+Q_0(T-T_\infty)-\frac{\partial q_r}{\partial y}+\sigma B_0^2u^2+(\mu(T)+\kappa)\left(\frac{\partial u}{\partial y}\right)^2 \tag{3}$$

Angular momentum equation

$$\rho j\left(\frac{\partial N}{\partial t}+u\frac{\partial N}{\partial x}+v\frac{\partial N}{\partial y}\right)=j\frac{\partial}{\partial y}\left(\left(\mu(T)+\frac{\kappa}{2}\right)\frac{\partial N}{\partial y}\right)-\delta\left(2N+\frac{\partial u}{\partial y}\right) \tag{4}$$

Mass transfer equation

$$\frac{\partial C}{\partial t}+u\frac{\partial C}{\partial x}+v\frac{\partial C}{\partial y}=D_m\frac{\partial^2 C}{\partial y^2}+\frac{D_mK_T}{T_m}\frac{\partial^2 T}{\partial y^2}-\frac{\partial(V_TC)}{\partial y} \tag{5}$$

The appropriate boundary conditions is presented [7 9] as

$$u=U_w(x,t)+L\frac{\partial u}{\partial y},\ v=0,\ N=0,\ T=T_w(x,t),\ C=C_w(x,t) \text{ at } \quad y=0 \tag{6}$$

$$u\to 0, N\to 0, T\to T_\infty, C\to C_\infty \quad \text{at} \quad y\to\infty \tag{7}$$

Where u and v are the components of velocity in x and y axis respectively, $C_p$is the specific heat at constant pressure and ρ is the fluid density. The vortex viscosity is denoted by κ, j is the microinertia density, δ is the spin-gradient viscosity. ϕ is the porosity of the porous medium, k_0 the permeability of the porous medium, ν is the kinematic viscosity, σ is the parameter denoting the electrically conductivity of the fluid, T is the dimensional fluid temperature. g is the gravitational acceleration, $\beta_{1,2}$ are the volumetric coefficients of the thermal expansion and volumetric expansion respectively. q_r is the radiative heat flux, C, C_w and C_∞ are the dimensional fluid concentration, surface concentration and the ambient concentration respectively. D_m is the coefficient of mass diffusitivity, T_m is the mean fluid temperature, K_T is the thermal diffusivity ratio.
Assuming that the temperature dependent viscosity $\mu(T)$ which varies as an exponential function of temperature of the form [36]

$$\mu(T)=\mu_\infty e^{\epsilon(T-T_\infty)} \tag{8}$$

where ϵ is the viscosity variation parameter and μ_∞ is the dynamic viscosity of the ambient fluid. The radiative heat flux q_r is employed according to the Rosseland diffusion approximation for radiation. For an Optically thick boundary layer the radiative heat flux is defined [27, 28] as

$$q_r=-\frac{4\sigma_1}{3\chi}\frac{\partial T^4}{\partial y}=\frac{16\sigma_1}{3\chi}T^3\frac{\partial T}{\partial y} \tag{9}$$

here σ_1 is the Stefan-Boltzman constant, χ is the mean absorption coefficient. Furthermore, the effect of thermophoresis is usually prescribed by the mean velocity, which a particle acquires when exposed to a temperature gradient in the y-direction. This is usually very much larger than in the x-direction, and therefore only the thermophoretic velocity in the y-direction is considered [9] and denoted by V_T. The thermophoretic velocity V_T in equation (5) is expressed [9] as follows

$$V_T = -\frac{\Delta\nu}{\mathrm{T_f}}\frac{\partial T}{\partial y} \tag{10}$$

In the above expression $\mathrm{T_f}$ and Δ are the temperature reference and thermophoretic coefficient with a range of values from 0.2 to 1.2. The thermophoretic coefficient Δ is defined [9, 13] as

$$\Delta = \frac{2c_s\left(\lambda_g/\lambda_p + c_s Kn\right)\left[1 + Kn\left(c_1 + c_2 e^{-(c_3/Kn)}\right)\right]}{(1 + 3c_r Kn)\left[1 + 2\,\lambda_g/\lambda_p + 2c_t Kn\right]} \tag{11}$$

where $c_1, c_2, c_3, c_r, c_s, c_t$ are constants, Kn is the Knudsen number, while λ_g and λ_p are the thermal conductivities of the fluid and the diffused particles respectively.

Following [20], we introduce the following similarity transformations,

$$u = \frac{ax}{1-ct}f'(\eta) = U_w f'(\eta), \qquad v = -\sqrt{\frac{a\nu}{1-ct}}f(\eta), \qquad N = \sqrt{\frac{a^3}{\nu(1-ct)^3}}x\,\omega(\eta),$$
$$T = T_\infty + \frac{bx}{\nu(1-ct)^2}\theta(\eta) = T_w\theta(\eta), \tag{12}$$
$$C = C_\infty + \frac{dx}{\nu(1-ct)^2}\phi(\eta) = C_w\phi(\eta), \qquad \eta = \sqrt{\frac{U_w(x,t)}{\nu x}}y.$$

Here $(')$ denotes the differentiation with respect to η. a, b, c, d are constants with dimension per time. The expressions for $U_w(x,t)$, $T_w(x,t)$ and $C_w(x,t)$ are valid for $t = 0$ or $t = c^{-1}$. Using equation (12) on equations (1) - (6), it is found that the continuity equation (1) is identically satisfied. Also making use of equations (8), (9) and (10) the momentum equation, angular momentum equation, heat balance equation and the concentration equation in dimensionless form yields respectively,

$$(e^{-\alpha\theta} + K)f''' - f''(\alpha\theta' - f) - (f')^2 - \frac{A}{2}(\eta f'' + 2f') + K\omega' - \left(H + \lambda e^{-\alpha\theta}\right)f' + Gr\theta + Gc\phi = 0 \tag{13}$$

$$\left(e^{-\alpha\theta} + \frac{K}{2}\right)\omega'' - \alpha\theta'\omega' + (f\omega' - f'\omega) - \frac{A}{2}(3\omega + \eta\phi') - KB(2\omega + f'') = 0 \tag{14}$$

$$\theta'' + Pr\left[(f\theta' - f'\theta) - \frac{A}{2}(4\theta + \eta\theta') + M(f')^2 + Ec(e^{-\alpha\theta} + K)(f'')^2\right] + \frac{4}{3N}\left((1 + \theta(T_r - 1)\theta)\theta'\right)' + Q\theta = 0 \tag{15}$$

$$\phi'' + Sc\left[(f\phi' - 2f'\phi) - \tau(\theta'\phi' + \theta''\phi) - \frac{A}{2}(\eta\phi' + 3\phi)\right] + ScSo\theta'' = 0 \tag{16}$$

$A = \frac{c}{b}$ is the unsteady parameter, $M = \frac{\sigma B_0^2}{\rho b}$ is the Hartmann number, $Pr = \frac{\mu_\infty C_p}{k}$ is the Prandtl number, $\delta = \frac{\nu\phi}{k_0 b}$ denotes the Porosity parameter, $T_r = \frac{T_w}{T_\infty}$ is the wall temperature excess ratio parameter, and the radiation parameter is denoted as $N = \frac{\chi k}{4\sigma {T_\infty}^3}$, $Gr = \frac{g\beta_1 b}{a^2}$ and $Gc = \frac{g\beta_2 b}{a^2}$ are the thermal Grashof number and solutal Grashof number parameters respectively. $Ec = \frac{{U^2}_w}{C_p(T_w - T_\infty)}$ is the Eckert number, $Sc = \frac{\nu}{D_m}$ is the Schmidt number, and $So = \frac{D_m K_T(T_w - T_\infty)}{\nu T_m(C_w - C_\infty)}$ is the Soret number, the thermophoretic parameter is denoted as $\tau = -\frac{\Delta(T_w - T_\infty)}{\mathrm{T_f}}$, $K = \frac{\kappa}{\mu_\infty}$ is the microrotation parameter, while $\alpha = \frac{\epsilon bx}{\nu(1-ct)^2}$ is the dimensionless variable viscosity parameter.

The corresponding dimensionless velocity slip, concentration slip and the convective boundary conditions are as follows

$$f'(\eta) = 1 + sf'', \ f(\eta) = 0, \ \omega(\eta) = 0, \ \theta(\eta) = 1, \ \phi(\eta) = 1 \quad \text{at} \quad \eta = 0 \tag{17}$$

$$f'(\eta) = 0, \quad \omega(\eta) = 0, \quad \theta(\eta) = 0, \ \phi(\eta) = 0 \qquad \text{at} \qquad \eta \to \infty \tag{18}$$

where the velocity slip parameter $s = L\sqrt{\frac{a}{\nu(1-ct)}}$. It is interesting to note that the model present study reduces to Singh and Kumar [7] in the absence of mass transfer and by letting $s = \alpha = Gc = k_0 = H = 0$ and $T_r = 1$. Physical quantities of practical interest in this problem are the local Skin friction coefficient C_{fx}, local wall couple stress coefficient M_{wx}, local Nusselt number Nu_x and local Sherwood number Sh_x which are defined as follows [6, 28].

$$
\begin{aligned}
C_{fx} &= \frac{2}{\rho {U_w}^2}\left((\mu(T)+\delta)\frac{\partial u}{\partial \eta}+\delta N\right)\Big|_{y=0} = 2\left(e^{-\alpha\theta}+K\right)f''(0),\\
M_{wx} &= \gamma\left(\frac{\partial N}{\partial y}\right)\Big|_{y=0} = \frac{\gamma a U_w}{\nu(1+ct)}\omega'(0)\\
Re_x^{-0.5}Nu_x &= \frac{x}{k(T_w-T_\infty)} - k\left[1+\frac{16\sigma}{3\chi k_\infty}T^3\right]\left(\frac{\partial T}{\partial y}\right)\Big|_{y=0} = \left(\left(1+\frac{4}{3N}\left(1+(T_r-1)\theta(\eta)\right)^3\right)\theta(\eta)\right)\theta'(\eta)\Big|_{\eta=0},\\
Re_x^{-0.5}Sh_x &= \frac{x}{D_T(C_w-C_\infty)} = -\phi'(\eta)|_{\eta=0}
\end{aligned}
\tag{19}
$$

where $Re_x^{0.5} = \frac{U_w(x,t)x}{\nu}$ is the local Reynolds number.

Numerical Solution

In order to solve the set of nonlinear differential equations (13) - (16), with the corresponding boundary conditions (17) and (18) numerically. The fourth-fifth order Runge-Kutta-Fehlberg integration scheme was used with the help of MAPLE algebraic package. In this method, the problem domain is discretized and the boundary conditions for $\eta = \infty$ are replaced by $f'(\eta_{max}) = 0$, $\omega'(\eta_{max}) = 0$, $\theta'(\eta_{max}) = 0$, and $\phi'(\eta_{max}) = 0$. The value of η_∞ is chosen to be a large value for which the boundary conditions in equation (18) are satisfied. Therefore η_∞ is replaced by η_{22} and the step size $\Delta\eta = 0.001$. The algorithm in MAPLE 18 package is strongly built and it has been well tested for its accuracy in [28, 35].

Numerical Result and Discussion

In this paper, the study of effects of variable viscosity, thermophoresis, Soret and thermal radiation on mixed convection flow of a micropolar fluid from an unsteady stretching surface with viscous dissipation and heat generation is carried out. The non-dimensional governing equations are transformed using the similarity transformation and are solved numerically using the fifth order Runge-Kutta-Fehlberg method (R.K.F M) along with shooting technique. The effect of dimensionless governing parameters on the flow, heat and mass transfer are discussed with the aids of graphs. The values of the skin friction coefficient, wall couple stress coefficient, local Nusselt number and Sherwood numbers are computed numerically in Table 2. In order to get the clear picture of the physical problem, the numerical results are obtained for different values of governing parameters for velocity, microrotation, temperature and concentration profiles. The default values used throughout the simulation are $Ec = 0.05$, $\lambda = 0.5$, $s = 0.1$, $H = 2$, $A = 0.5$, $R = 0.5$, $Pr = 0.72$, $K = 0.2$, $Gr = 0.2$, $Gc = 0.2$, $\alpha = 0.5$, $Q_0 = 0.1$, $Sc = 0.2$, $So = 0.1$, $\tau = 0.2$, and $T_r = 2$.

Code Validation

In to order validate the accuracy of the present code, the non-dimensional governing equations (13) – (16) with the corresponding boundary conditions (17) – (18) are reduced to the corresponding set of equations governing the problem in [6] in the absence of mass transfer, MHD porous medium, and non-linear thermal radiation. The results obtained from the reduced equation were compared with those obtained in [6] as shown in Table 1. It is seen that the results agree well for the set of varying parameters and hence justify the use of the code for this present model.

The dimensionless velocity for various values of porous medium parameter λ and velocity slip parameter s are presented in Fig 2. The velocity profile decreases with increase in porous medium parameter λ. This is as a result of the fact that the presence of porous medium enhances the resistive (drag) force motion which in turns decelerates the velocity and the angular velocity fields in the boundary layer. It is shown from the same plot that increasing the velocity slip parameter s decelerates the flow in the boundary layer.

Fig 3 depicts the velocity profile for different values of Hartmann number H. It is observed that an increase in Hartmann number decreases the velocity distribution profile. Also the momentum boundary layer thickness decreases as parameter H increases. The reason behind this trend is the force produced by the applied magnetic field normal to the fluid. This force called Lorentz force acts in opposite direction to the flow and hence results in decreasing the velocity profile. The effect of varying values of variable viscosity parameter α is also illustrated in the same figure. It is seen that variable viscosity parameter α increases the velocity profile. This is because increasing variable viscosity parameter α reduces the fluid viscosity. The fluid's resistance to flow therefore reduces which in turns enhances the fluid velocity.

Figs 4 and 5 present the influence of solutal Grash of number Gc and thermal Grashof number Gr on velocity and microrotation (angular velocity) profiles respectively. It is observed in both cases that an upward acceleration of the fluid in the vicinity of the vertical wall is noticed with increasing intensity of buoyancy forces. Also in Fig 6, Effect of Hartmann number H and variable viscosity parameter α on the microrotation profile is shown. Observations similar to Fig 4 are noticed. The dimensionless velocity for various values of porous medium parameter λ and velocity slip parameter s are depicted in Fig 7. The microrotation profile decreases with increase in porous medium parameter λ. The presence of porous medium enhances the resistive (drag) force motion which in turns decelerates the velocity and the angular velocity fields in the boundary layer. It is shown from the same plot that increasing the velocity slip parameter s accelerates the flow in the boundary layer.

Fig 8 depicts the variation of micropolar parameter K and the unsteadiness parameter A on the microrotation profile. It is observed in this figure that the maximum point is shifted to the surface as the values of K is increased. While increase in the unsteadiness parameter A causes a decrease in the microrotation profile. In Fig 9, effects of Hartmann number H and variable viscosity α on concentration profile are depicted. It is seen that the concentration profile is increased as the values of Hartmann number H and variable viscosity parameter α are increased.

The effects of thermophoretic parameter τ and unsteadiness parameter A on concentration profile are depicted in Fig 10. It found that increasing the thermophoretic parameter τ causes a decrease in the concentration profile thereby reducing the concentration boundary layer thickness. The unsteadiness parameter Adecreases the thermal boundary layer thickness as well.

Table 2: demonstrate the effect of the unsteadiness parameter A, the thermal radiation parameter R, the micropolar parameter K, the Soret number parameter So and the thermophoretic parameter τ on the local skin-friction coefficient $(-f''(0))$, local wall couple stress coefficient $(-\omega'(0))$, local Nusselt number $(-\theta(0))$ and the local Sherwood number $(-\phi(0))$ with other parameters fixed. It is seen from the table that local wall couple stress coefficient $(-\omega'(0))$ increase with an increase in parameters $\tau, K,$ and R. But reduces on increasing the values of So and A. In addition, the values of $-f''(0)$, $-\phi(0)$ and $-\theta(0)$ increase by increasing the values of unsteadiness parameter A, while a reverse is noticed for the case of $-\omega'(0)$. Further, the rate of heat transfer at the surface $(-\theta(0))$ decreases with an increase in τ, while the local Sherwood number $(-\phi(0))$ increases for an increasing values of τ.

Effects of varying values of Schmidt number Sc and Soret number So on the concentration profile is illustrated in Fig 11. It is observed that the concentration profile decreases as Sc increases. This causes a reduction in the concentration boundary layer thickness. While reverse effect is noticed when parameter So is increased as shown in Fig 11.

Fig 12 and 13 illustrate the effects of solutal Grashof number and thermal Grashof number Gr on concentration and temperature profiles respectively. As reported in Fig 4 and 5, a downward trend is observed. Influences of thermal radiation parameter R and temperature ratio parameter T_r on temperature profile are depicted in Fig 14. It is shown from this plot that increasing parameter Rdecreases the temperature profile. This result is same as that reported by Singh and Kumar [7]. It can be seen that the thermal boundary layer thickness decreases as parameter R increases. This increases the absolute value of the temperature gradient at the surface. It is also observed from the same figure that the thermal radiation parameter R reduces for non-linear thermal radiation $(T_r = 2)$when compared with that of the linear thermal radiation $(T_r = 1)$. It is remarked that the thermal boundary layer becomes thinner for non-linear than that of the linear thermal radiation.

Fig 15 illustrates temperature profiles for different values of Hartman number H and variable viscosity parameter α. Increase in Hartman number increases the temperature profile. The increment in the temperature profile is due to the effect of Lorentz force which generates flow friction. This friction thereby generates heat energy which enhances the flow temperature. The temperature profile also increases with an increase in variable viscosity parameter α, resulting in an increase in the thermal boundary layer thickness.

Effect of variation in Prandtl and Eckert numbers (Pr and Ec) on the temperature profile are displayed in Fig. 16. Increase in Prandtl number decrease the temperature profile. As Prandtl number increases the thermal diffusivity become lower, this results to reduction in the thickness of the boundary layer. It is shown also from the same plot that Eckert number increases the temperature profile. This is due to the fact that increasing Eckert number allows energy to be stored in the fluid region as a result of viscous dissipation. In Fig 17, effect of varying values of heat source parameter Q_0 and unsteadiness parameter A on temperature profile is depicted. Increasing the value of Q_0 increases the temperature profile. It is seen that the temperature profile increases as the heat source parameter Q_0 generates energy which causes rise in the fluid temperature. The unsteadiness parameter A monotonically decreases the temperature profile.

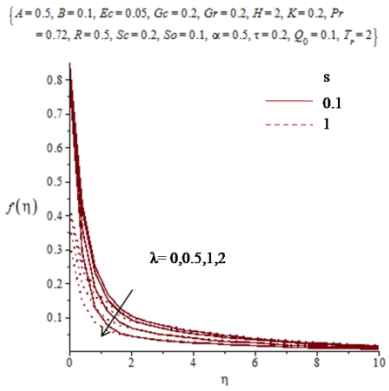

Fig 2 Effects of λ and s on velocity profile.

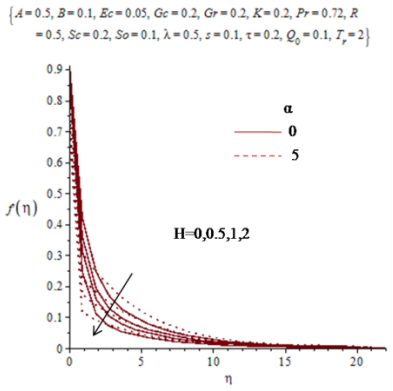

Fig 3 Effects of H and α on velocity profile.

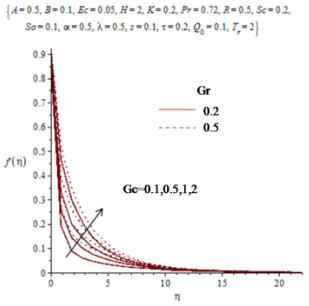

Fig 4 Effects of Gc and Gr on velocity profile.

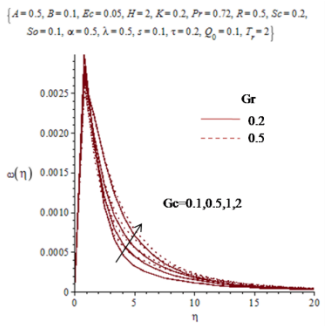

Fig 5 Effects of Gc and Gr on microrotation profile.

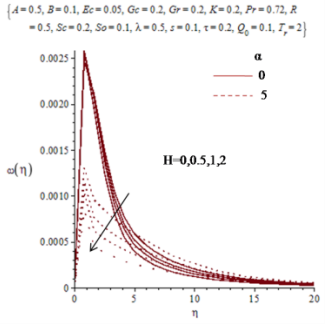

Fig 6 Effects of H and α on microrotation profile.

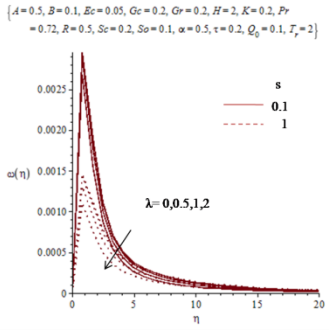

Fig 7 Effects of λ and s on microrotation profile.

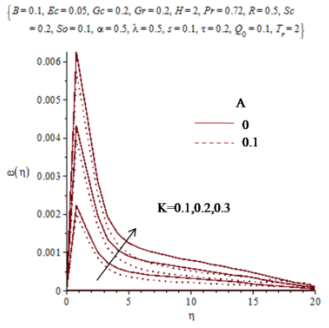

Fig 8 Effects of K and A on microrotation profile.

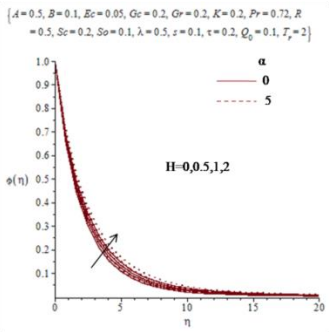

Fig 9 Effects of H and α on concentration profile.

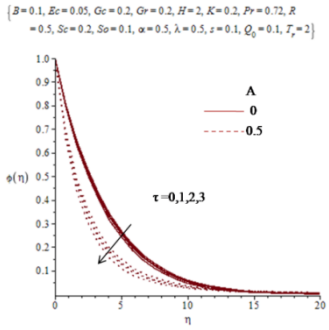

Fig 10 Effects of τ and A on concentration profile.

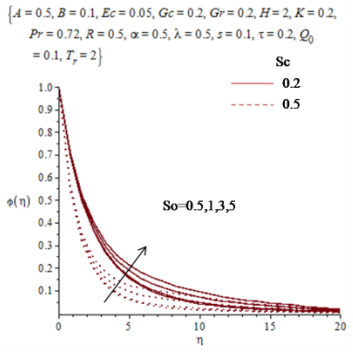

Fig 11 Effects of So and Sc on concentration profile.

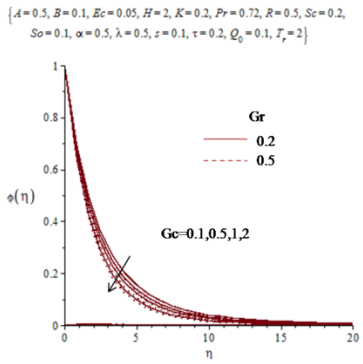

Fig 12 Effects of Gc and Gr on concentration profile.

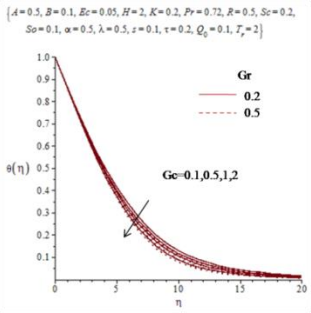

Fig 13 Effects of Gc and Gr on temperature profile.

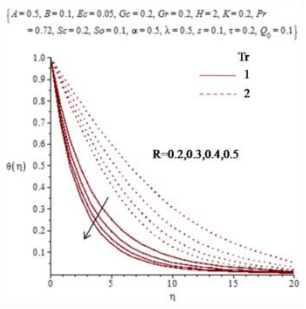

Fig 14 Effects of R and T_r on temperature profile.

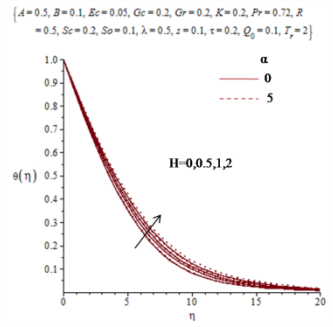

Fig 15 Effect of H and α on temperature profile.

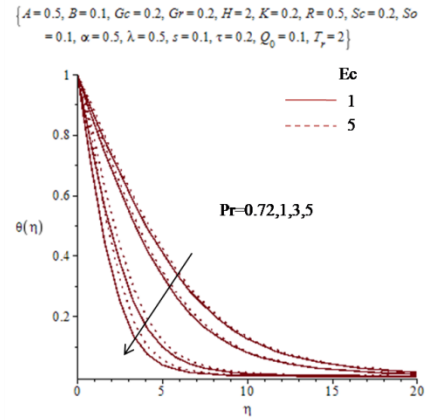

Fig 16 Effects of Pr and Ec on temperature profile.

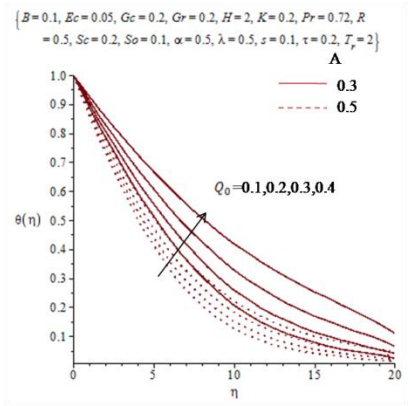

Fig 17 Effects of Q_0 and A on temperature profile.

Conclusion

In this paper, we have numerically investigated the effects of variable viscosity, thermophoresis, Soret, heat source and nonlinear thermal radiation on unsteady MHD micropolar fluid in a porous medium with ohmic heating. The governing partial differential equations are reduced into a set of nonlinear ordinary differential equations using similarities transformations. The reduced equations are solved numerically using Fehlberg fourth order Runge-Kutta method. The following observations and conclusions are drawn

1) Increase in porous parameter and velocity slip parameter causes a decrease in the momentum boundary layer thickness.

2) The velocity profile tends to decrease with an increase in magnetic parameter while temperature and concentration profile reduces with increase in magnetic parameter, respectively.
3) Increase in nonlinear thermal radiation parameter decelerates the fluid temperature.
4) The Sherwood number increases with an increase in Soret number while the rate of mass transfer decrease with an increase in porous parameter.
5) The concentration boundary layer becomes thinner with an increase in thermophoretic parameter.
6) The concentration boundary layer decreases with an increase τ, while the local Sherwood number increases with increasing values of τ.

Table 1: Numerical values of $-f''(0)$, $-\theta'(0)$ and $-\omega'(0)$ for different values of A, K, Gr, R.

Singh and Kumar [7]							*Present result*		
A	Gr	K	R	$-f''(0)$	$\omega'(0)$	$-\theta'(0)$	$-f''(0)$	$\omega'(0)$	$-\theta'(0)$
0	0	0.2	0.5	0.91248	0.027431	0.36217	0.91219018	0.02739408	0.32482125
0.2	0	0.2	0.5	0.97460	0.024750	0.45577	0.97434740	0.02472270	0.44754438
0.2	0.05	0.2	0.5	0.94316	0.023959	0.46128	0.94144039	0.02382086	0.45482396
0.2	0.1	0.2	0.5	0.91260	0.023225	0.46628	0.91002480	0.02302229	0.46099704

Table 2: Numerical values of $-f''(0)$, $-\theta'(0)$, $-\omega'(0)$, $-\phi'(0)$ for different values of A, τ, K, R, So when $\alpha = h = 0$.

A	τ	K	R	So	$-f''(0)$	$-\omega'(0)$	$-\theta'(0)$	$-\phi'(0)$
0	0.2	0.2	0.5	0.1	1.565133	0.034507	0.023513	0.310673
0.2					1.616755	0.031959	0.083518	0.393471
0.4					1.663936	0.029989	0.118604	0.462090
0.5	0	0.2	0.5	0.1	1.688638	0.029170	0.132783	0.489453
	0.2				1.686486	0.029174	0.132778	0.492222
	0.5				1.686648	0.029179	0.132771	0.496404
0.5	0.2	0	0.5	0.1	1.861172	0	0.485835	0.133069
		0.1			1.767489	0.015023	0.489161	0.132923
		0.3			1.615497	0.042558	0.495056	0.132636
0.5	0.2	0.2	0.2	0.1	1.684343	0.029061	0.084894	0.492602
			0.5		1.686486	0.029174	0.132778	0.492222
			1		1.688776	0.029291	0.184366	0.491825
0.5	0.2	0.2	0.5	0.1	1.686486	0.029173	0.132778	0.492222
				0.2	1.686464	0.029173	0.132780	0.491917
				0.3	1.686442	0.029172	0.132783	0.491613

Conclusion

In this paper, we have numerically investigated the effects of variable viscosity, thermophoresis, Soret, heat source and nonlinear thermal radiation on unsteady MHD micropolar fluid in a porous medium with ohmic heating. The governing partial differential equations are reduced into a set of nonlinear ordinary differential equations using similarities transformations. The reduced equations are solved numerically using Fehlberg fourth order Runge-Kutta method. The following observations and conclusions are drawn

1) Increase in porous parameter and velocity slip parameter causes a decrease in the momentum boundary layer thickness.
2) The velocity profile tends to decrease with an increase in magnetic parameter while temperature and concentration profile reduces with increase in magnetic parameter, respectively.
3) Increase in nonlinear thermal radiation parameter decelerates the fluid temperature.
4) The Sherwood number increases with an increase in Soret number while the rate of mass transfer decrease with an increase in porous parameter.
5) The concentration boundary layer becomes thinner with an increase in thermophoretic parameter.
6) The concentration boundary layer decreases with an increase τ, while the local Sherwood number increases with increasing values of τ.
7) **Table 1: Numerical values of $-f''(0)$, $-\theta'(0)$ and $-\omega'(0)$ for different values of** A, K, Gr, R.

Singh and Kumar [7]							*Present result*		
A	Gr	K	R	$-f''(0)$	$\omega'(0)$	$-\theta'(0)$	$-f''(0)$	$\omega'(0)$	$-\theta'(0)$
0	0	0.2	0.5	0.91248	0.027431	0.36217	0.91219018	0.02739408	0.32482125
0.2	0	0.2	0.5	0.97460	0.024750	0.45577	0.97434740	0.02472270	0.44754438
0.2	0.05	0.2	0.5	0.94316	0.023959	0.46128	0.94144039	0.02382086	0.45482396
0.2	0.1	0.2	0.5	0.91260	0.023225	0.46628	0.91002480	0.02302229	0.46099704

Table 2: Numerical values of $-f''(0)$, $-\theta'(0)$, $-\omega'(0)$, $-\phi'(0)$ for different values of A, τ, K, R, So when $\alpha = h = 0$.

A	τ	K	R	So	$-f''(0)$	$-\omega'(0)$	$-\theta'(0)$	$-\phi'(0)$
0	0.2	0.2	0.5	0.1	1.565133	0.034507	0.023513	0.310673
0.2					1.616755	0.031959	0.083518	0.393471
0.4					1.663936	0.029989	0.118604	0.462090
0.5	0	0.2	0.5	0.1	1.688638	0.029170	0.132783	0.489453
	0.2				1.686486	0.029174	0.132778	0.492222
	0.5				1.686648	0.029179	0.132771	0.496404
0.5	0.2	0	0.5	0.1	1.861172	0	0.485835	0.133069
		0.1			1.767489	0.015023	0.489161	0.132923
		0.3			1.615497	0.042558	0.495056	0.132636
0.5	0.2	0.2	0.2	0.1	1.684343	0.029061	0.084894	0.492602
			0.5		1.686486	0.029174	0.132778	0.492222
			1		1.688776	0.029291	0.184366	0.491825
0.5	0.2	0.2	0.5	0.1	1.686486	0.029173	0.132778	0.492222
				0.2	1.686464	0.029173	0.132780	0.491917
				0.3	1.686442	0.029172	0.132783	0.491613

References

[1] B C Sakiadis. Boundary layer behavior on continuous solid surface. *AIChE J.* 1961; **7**, 26-8

[2] L Crane. Flow past a stretching sheet. *Z Angew Math Phy.s* 1970; **21**,645-7

[3] A.C Eringen. Theory of micropolar fluid. *J. Math. Mech.* 1966; **16**,1-18

[4] M.W Heruska, L.T Watson, and K.K Sankara. Micropolar fluid past a porous stretching sheet. *Computer and fluids.* 1986; **14(2)**, 117-129

[5] M.M Rahman, M.A Rahman, M.A Samad, M.Salam. Heat transfer in micropolar fluid along a linear stretching sheet with temperature dependent viscosity and variable surface temperature. *Int. J. Thermmophys.* 2009; **30**, 1649-1670

[6] K. Singh and M. Kumar. The effect of chemical reaction and double stratification on MHD free convection in a micropolar fluid with heat generation and Ohmic heating. *Jordan Journal of Mechanical and Industrial Engineering.* 2015; **9(4)**, 279-288
[7] K Singh and M kumar. Effect of thermal radiation in mixed convention of a micropolar fluid from an unsteady stretching surface with viscous dissipation and heat generation/absorption. *International journal of chemical Engineering*. 2016 Article ID 8190234 10 pages. doi.org/10.1155/2016/81/90234
[8] M Turyilmazoglu. Flow of a micropolar fluid due to porous stretching sheet and heat transfer. *International Journal of Non-linear Mechanics.* 2016; **83**, 59-64
[9] A. Zaib and S. Shafie. Heat and mass transfer in a MHD non-Dacian micropolar fluid over an unsteady starching sheet with non-uniform heat source/sink and thermophoresis. *Heat transfer-Asian research* 2012; Doi.1002/htj.21018
[10] K Das. Effect on MHD mixed convection stagnation point flow of a micropolar fluid towards a shrinking vertical sheet. *Computers and mathematica with application*. 2012; **63**, 255-267
[11] A Zaib and S Shafie. Slip effect on unsteady MHD stagnation-point flow of a micropolar fluid towards a shrinking sheet with thermophoresis effect. *International journal for computational method in engineering science and mechanics* 2015; **16**, 285-291
[12] M B Ashraf, T Hayat, S A Shehzad, and B Ahmed. Thermophoresis and MHD mixed convection three dimensional flow of viscous elastic fluid with Soret and Dufour effects. *Neural Comput and Applic.* DOI 10.1007/s00521-017-2997-5
[13] L Talbot, R K Chenge, A W Schefer and D R Willis.Thermophoresis of particles in a heated boundary layer. J. Fluid Mech. 1980; **101,** 737-758
[14] C J Tsai, J S Lin, I Shankar, G Aggarwal and D R. Chen. Thermophoresis deposition of particles in laminar and turbulent tube flows. *Aerosol sin, technol.* 2004; **338**,131-139
[15] A J Chamkha and I. Pop. Effect of thermophoresis particle deposition in free convection bondary layer from a vertical flat plate embedded in a porous medium. Int. comm. *International journal of heat and mass transfer* 2004; **31**, 421-430
[16] J Zueco, O. A Beg and L M Lopez-Ochoa. Effect of thermophoresis particle deposition and the thermal conductivity in a porous plate with dissipative heat and mass transfer. *Acta Mech. Sin.* 2011; **27**, 389-398
[17] R Alouaoul and M N Bouaziz. Influence of thermophoresis on MHD micropolar fluid over a moved permeable plate. *mechanika* 2017; **23(3)**, 382-390
[18] N.F.M Noor. Analysis for MHD flow of Maxwell fluid past a vertical stretching sheet in the presence of thermophoresis and chemical reaction. *World Academic of science Engineering and technology.* 2012; **64**, 1019-1023
[19] S Shateyi. A new mechanical approach to MHD flow of a Maxwell fluid past a vertical stretching sheet in the presence of thermophoresis and chemical reaction. *Boundary value problems.* 2013:196
[20] K Das. Influence of thermophoresis and chemical reaction on MHD micropolar fluid with variable fluid properties. *International journal of heat and mass transfer* 2012; **55**,7166-7174
[21] M A Saddeek. Finite element method for effect of chemical reaction, variable viscosity, thermophoresis and heat and mass transfer over a heat surface. *Acta Mechanica*. 2005; **177**, 1-18
[22] R A Mohamed and S M Abo-Dahab. Influence of chemical reaction and thermal radiation on heat and mass transfer in MHD micropolar flow over a vertical moving porous plate in a porous medium with heat generation. *International Journal of thermal Sciences.* 2009; **48,** 1800-1813
[23] M Madhu, N Kishan and A J Chamkha. Unsteady flow of a Maxwell nanofluid over a stretching surface in the presence of magnetohydrodynamic and thermal radiation effects. *Propulsion and power research* 2017; **6(1),** 31-40
[24] D Prakash and M Muthtamilselvan. Effect of radiation on transient MHD flow of micropolar fluid between porous vertical channel with boundary condition of the third kind. *Ain Shams Engineering Journal.* 2014; **5(4),** 1277-1286
[25] K Bhattacharyya, S Mukhopadhyay, G C Layek and I Pop. Effect of thermal radiation on micropolar fluid flow and heat transfer over a porous shrinking sheet. *International journal of heat and mass transfer.* 2012; **55(11),** 2945-2952
[26] A S Idowu, M S Dada, O T Babalola, T A **Yusuf,** and E B Are. DTM-Pade solution for Heat transfer of hydro magnetic flow over a vertical plate. *Journal of Nigerian Association of Mathematical Physics*, 2016; **36**, 153-162
[27] C K Chen, Y T Yang and K H Chang. The effect of thermal radiation on entropy generation due to micropolar fluid flow along a wavy surface. *Entropy*. 2011; **13**, 1595-1610
[28] Uddin M.J, Beg O.A, Ismail A.I. Radiative convective nanofluid past a starching/shrinking sheet with slip effects. *Journal of thermophysics and heat transfer. (2015) DOI:10.2514/1.T4372*.
[29] T A Yusuf and T M Ashiru. Variable thermal conductivity and nonlinear thermal radiation on MHD Oldroyd-B fluid in a porous channel with stretching walls. Proceeding of the 54th Annual Conference, (Mathematics Science) Nigeria. 2017, p. 1-8
[30] J A Gbadeyan and T A Yusuf. Second Law Analysis of Radiative Unsteady MHD fluid flow with partial slip and convective cooling. *Asian journal of Mathematics and Computer Research.* 2017; **17(4),** 212-236
[31] F Maboob, S M Ibrahim, M M Rashidi, M S Shadloo, and G Lorenzini. Non-uniform heat source/sink and Soret effect on MHD non Darcian convective flow past a stretching sheet in a micropolar fluid with radiation. *International Journal of Heat and Mass Transfer*. 2016; **93**, 674-682
[32] A Zaib, R.M Kasin, N.F Mohammed and S.Shafie. Soret and Dufour effect on unsteady MHD flow of a micropolar fluid in the presence of thermophoresis deposition particle. *World Appl.sci*. 2013; **21**, 766-773
[33] M.K Partha. Suction/injection effect of thermophoresis particle deposition in a non-Darcy porous medium under the influence of Soret and Dufour effects. *International journal of heat and mass transfer.* 2008; **44**, 969-977
[34] T Hayat, S A Shehzad A Alsaedi Soret and Dufour effect in the manetohydrodynamic (MHD) flow of Casson fluid. *Appl Math Mech Engl Ed.* 2012; **33**, 1301-1312
[35] B J Gireeha, B Mahanthesh, P T Manjunatha, R S R Gorla. Numerical solution for hydromagnetic boundary layer flow and heat transfer past a stretching surface embedded in non-Darcy porous medium with fluid-particle suspension *Journal of Nigerian Mathematical society* 2015; **34**, 267-285
[36] T Chinyoka and O D Makinde. Buoyancy effects on Unsteady MHD flow of a reactive third-grade fluid with asymmetric convective cooling. *Journal of Applied Mechanics.* 2015; **8(4),** 931-941